






Investigation of the carbon monoxide dication lifetime using $(\text{CO})_2$ dimer fragmentationA. Méry ¹, X. Flécharde ^{2,*}, S. Guillous,¹ V. Kumar ^{1,3}, M. Lalande,¹ J. Rangama,¹ W. Wolff ⁴ and A. Cassimi ¹¹*CIMAP, CEA, CNRS, ENSICAEN, UNICAEN, Normandie Université, BP5133, 14050 Caen Cedex 04, France*²*LPC Caen, ENSICAEN, UNICAEN, CNRS, IN2P3, Normandie Université, 14000 Caen, France*³*Inter University Accelerator Center, Aruna Asaf Ali Marg, New Delhi, Delhi 110067, India*⁴*Instituto de Física, Universidade Federal do Rio de Janeiro, Cidade Universitária, Rio de Janeiro 21941-909, Brazil*

(Received 22 July 2021; revised 7 October 2021; accepted 8 October 2021; published 21 October 2021)

The fragmentation of carbon monoxide dimers induced by collisions with low-energy Ar^{9+} ions is investigated using the cold target recoil ion momentum spectroscopy technique. The presence of a neighbor molecule in the dimer serves here as a diagnostic tool to probe the lifetimes of the CO^{2+} molecular dications resulting from the collision. The existence of metastable states with lifetimes ranging from 2 ps to 200 ns is clearly evidenced experimentally through a sequential three-body fragmentation of the dimer, whereas fast dissociation channels are observed in a so-called concerted three-body fragmentation process. The fast fragmentation process leads to a kinetic energy release distribution also observed in collisions with monomer CO targets. This is found in contradiction with the conclusions of a previous study attributing this fast process to the perturbation induced by the neighbor molecular ion.

DOI: [10.1103/PhysRevA.104.042813](https://doi.org/10.1103/PhysRevA.104.042813)**I. INTRODUCTION**

Doubly charged diatomic molecular ions have unusual properties leading to a wide range of lifetimes against dissociation. Their stability depends on both the accessible decay mechanisms and the position of the populated rovibronic levels with respect to the barrier height. Among the large variety of doubly charged diatomic species investigated so far, CO^{2+} is probably the one that has attracted the largest interest, with measured lifetimes ranging from submicroseconds to a few seconds. Since its first observation within a mass spectrometer [1], the lifetime of metastable states of CO^{2+} has been widely studied both experimentally and theoretically. The existence of excited states with lifetimes in the millisecond range and up to a few seconds has been demonstrated using an ion storage ring [2]. Shorter lifetimes in the 10 ns to 1 μs range have also been identified [3,4]. In parallel, computational studies have shown that only the lowest vibronic levels ($v \leq 3$) of the electronic ground state ($^3\Pi$) and low-lying states ($^1\Sigma^+$, $^1\Pi$, and $^3\Sigma^+$) of CO^{2+} have lifetimes longer than 1 ns [5–7]. The decay rate of these states was found to be mainly governed by tunneling or by predissociation to the repulsive $^3\Sigma^-$ state [8].

More recently, a fast dissociation channel of the CO^{2+} molecular dication has been observed in the three-body breakup of triply charged dimers $(\text{CO})_2^{3+}$ ionized by intense ultrashort laser pulses [9]. However, this fast process was found to be associated with a higher kinetic energy release (KER) distribution than expected when compared to the dissociation of the isolated CO^{2+} molecular ion. The authors suggested that this fast process would only exist in a van der Waals complex due to the weak coupling with a neighbor CO^+ molecular ion. The symmetry breaking induced by the coun-

tercharge then leads to an avoided crossing with a dissociation channel, whereas the monomer would dissociate only via a weaker spin-orbit coupling.

In the present work we revisit this investigation using Coulomb explosion imaging (CEI) of triply charged $(\text{CO})_2^{3+}$ dimers ionized by low-energy Ar^{9+} ions. The presence of a neighbor molecular CO^+ ion serves here as a probe to get insight into the dissociation process of the other CO^{2+} molecular ion resulting from the collision. The detailed study of the kinematic of the three-body fragmentation channel provides a clear signature of the lifetime ranges of the CO^{2+} dication for several sets of data. The corresponding KER distributions are then used to identify the states of the CO^{2+} molecular ion initially populated by the collision process. This investigation differs from the work of [9] by two aspects: (i) the use of low-energy highly charged ions as projectiles, which leads to multiple electron capture from the target and to the population of states with higher excitation energy, and (ii) a higher momentum resolution, which allows a clearer comparison with the dissociation of isolated CO^{2+} molecular ions.

II. EXPERIMENT

The cold target recoil ion momentum spectroscopy (COLTRIMS) setup used for this work has already been described in detail elsewhere [10]. We thus only provide here a brief description of the method and of the experimental conditions. The 135-keV Ar^{9+} projectile beam was sent to the experiment through the ARIBE/GANIL facility. After beam collimation by a 600- μm aperture, the projectile ions collided with a supersonic gas jet target composed of $\sim 99\%$ CO molecules (monomers) and $\sim 1\%$ $(\text{CO})_2$ dimers. The scattered projectiles were charge selected using a set of deflection plates combined with a position-sensitive detector. The fragments of the ionized targets were collected on a second 80-mm-diam

*flecharde@lpccaen.in2p3.fr

position-sensitive detector due to a 40-V/cm electric field. The position and time of flight (TOF) of each fragment allowed then the identification of their mass-over-charge ratio and the three-dimensional reconstruction of their momentum in the center of mass of the molecular complex. As reported in [10], special care has been devoted to the clean selection of the different dissociation channels, to the calibration of the kinetic energy released in the fragmentation, and to the optimization of the energy resolution.

III. RESULTS AND DISCUSSION

Three different fragmentation channels will be discussed. On one hand, the removal of three electrons from a $(\text{CO})_2$ dimer target can lead to the two-body dissociation channel $(\text{CO})_2^{3+} \rightarrow \text{CO}^{2+} + \text{CO}^+$ or to the three-body one $(\text{CO})_2^{3+} \rightarrow \text{CO}^+ + \text{C}^+ + \text{O}^+$. From both channels, information on the lifetime of the states of the transient CO^{2+} dication can be extracted. On the other hand, the fragmentation of isolated CO^{2+} dications resulting from collisions with monomers $\text{CO}^{2+} \rightarrow \text{C}^+ + \text{O}^+$ was conjointly studied to serve as a reference for momentum calibration and to be compared with the dissociation of CO^{2+} observed within a $(\text{CO})_2$ dimer target.

A. Experimental results and access to the CO^{2+} lifetime

The two-body $(\text{CO})_2^{3+} \rightarrow \text{CO}^{2+} + \text{CO}^+$ dissociation channel is found to contribute to about 7% of the relaxation of triply charged $(\text{CO})_2^{3+}$ dimers. Since the TOF of the CO^{2+} molecular ion in the spectrometer is about $2.7 \mu\text{s}$, this channel arises from the population of metastable states with lifetimes that are larger or comparable. Its low relative intensity results mainly from the low proportion of such metastable states of the CO^{2+} dication in comparison with states of shorter lifetime leading to the competing three-body channel $(\text{CO})_2^{3+} \rightarrow \text{CO}^+ + \text{C}^+ + \text{O}^+$. The experimental observables do not allow a direct identification of these very-long-lived states that can most probably be assigned to the lowest vibration levels ($\nu = 0, 1$) of the $^3\Pi$ and $^1\Sigma^+$ state of the CO^{2+} dication [6].

The three-body $(\text{CO})_2^{3+} \rightarrow \text{CO}^+ + \text{C}^+ + \text{O}^+$ channel is more interesting as the sharing of the kinetic energy between the three fragments carries information on both the lifetime and the initial state of the CO^{2+} dication. For $(\text{CO})_2^{3+}$ [9] and $(\text{CO}_2)_2^{3+}$ [11], a detailed analysis of the three-body fragmentation dynamics was already performed using a momentum selection of the singly charged molecular ion combined with a Newton representation of the fragments momenta. We use here a slightly different method based on Dalitz plots which provides a more direct selection of different typologies of fragmentation dynamics. Figure 1(a) shows the experimental Dalitz diagram of the three-body dissociation of the dimer. This two-dimensional graph represents the reduced squared momenta of each fragment $\varepsilon_i = \frac{p_i^2}{\sum_{i=1}^3 p_i^2}$ (where the subscript i stands for the C^+ , O^+ , and CO^+ recoiling ions) along the three axes of the diagram (shown as dotted lines). The corresponding Cartesian coordinates are calculated as $x_D = \frac{\varepsilon_1 - \varepsilon_2}{\sqrt{3}}$ for the horizontal scale and $y_D = \varepsilon_3 - \frac{1}{3}$ for the vertical scale, where i is the number of the fragment sorted in ascending order of mass-to-charge ratio.

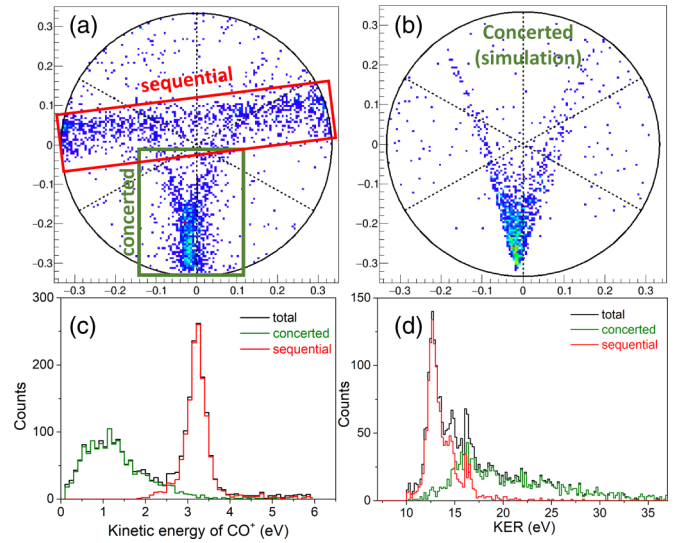


FIG. 1. Identification of the concerted and sequential fragmentation processes in the $(\text{CO})_2^{3+} \rightarrow \text{CO}^+ + \text{C}^+ + \text{O}^+$ dissociation channel. (a) Dalitz diagram of experimental data indicating the selection windows for concerted and sequential dissociation. (b) Dalitz diagram obtained by numerical simulation for concerted fragmentation events [10]. (c) Kinetic energy of the CO^+ molecular ion for concerted [green (light gray) line] and sequential [red (gray) line] events. (d) Total KER of the three-body fragmentation for concerted [green (light gray) line] and sequential [red (gray) line] events.

Several features are observed in Fig. 1(a): for $y_D < 0$, a dense region at the bottom of the vertical axis followed by a V-shape tail and for $y_D > 0$ a quasi-horizontal band. Events with $y_D < 0$ correspond to a simultaneous breakup of both the covalent and van der Waals bonds and will be referred to as concerted fragmentation events. The exact distribution of these events is directly correlated to the dissociation dynamics of the CO^{2+} dication but also to the initial structure of the dimer. In a previous study [10] assuming a simultaneous three-body breakup, Monte Carlo (MC) simulations have shown that the lowest part of the Dalitz plot with its V-shape distribution can be almost perfectly reproduced by the prompt three-body fragmentation of a CO dimer whose initial angles between the van der Waals bond and the covalent bonds are randomly distributed. This quasi-isotropic orientation was found to result from the low-energy barrier between several conformers of the dimer and from the finite temperature of the gas jet. The Dalitz plot obtained in [10] by MC simulation for this fast fragmentation process is shown in Fig. 1(b) for comparison.

Contrarily, the quasi-horizontal band in the upper part of the graph is associated with a sequential fragmentation. In the first step, Coulomb repulsion within the triply ionized dimer leads to the fast breakup of the van der Waals bond. This breakup is then followed by a delayed dissociation of the metastable CO^{2+} dication occurring when both covalent molecular ions have reached their asymptotic kinetic energy. Note that these events can only be observed if the fragmentation occurs at a shorter time than the $2.7\text{-}\mu\text{s}$ TOF of the CO^{2+} ions. The density distribution of the sequential events is localized close to the edge of the Dalitz graph. This is the signature of an in-plane dissociation: Before fragmenting, the $(\text{CO})^{2+}$ rotates

in the initial plane containing the center of mass of the CO^+ ion and the axis of the $(\text{CO})^{2+}$ dication. Such a rotation in the initial plane was recently reported in the sequential three-body fragmentation of triatomic molecules [12]. Here we observe a very similar behavior in the two-step dissociation of noncovalent molecular dimers.

Figure 1(c) shows the kinetic energy of the CO^+ ion for the selection windows of the Dalitz plot corresponding to sequential and concerted events. As previously observed for the fragmentation of $(\text{CO})_2^{3+}$ [9] and of $(\text{CO}_2)_2^{3+}$ [11] dimers, the distributions associated with a concerted or with a sequential dissociation are clearly different. The energy of the main peak at 3.2 eV (in red) corresponds to half the Coulomb potential energy of the transient dissociating $\text{CO}^+ + \text{CO}^{2+}$ system and is a clear signature of a sequential fragmentation. In such a two-step fragmentation process, the CO^{2+} dication breaks up only after the two recoiling molecular ions have reached the asymptotic limit for which their relative Coulomb repulsion vanishes. The CO^+ ion thus acquires the exact same kinetic energy as in the two-body channel $(\text{CO})_2^{3+} \rightarrow \text{CO}^{2+} + \text{CO}^+$, i.e., 3.2 eV [10]. The existence of metastable states of the CO^{2+} molecular dication is thereby experimentally and easily evidenced due to the presence of the second neighbor molecule in the dimer. This is in striking contrast with what has been previously obtained using the same experimental technique for $(\text{N}_2)_2$ dimers, where no sign of such a two-step process could be observed [13]. The lower part of the CO^+ energy spectrum (green line) corresponds to the concerted fragmentation where the CO^{2+} dication dissociates within a much shorter timescale. In this case, the CO^+ acquires a lower kinetic energy because of the fast repulsion of the two C^+ and O^+ atomic ions following the dissociation of the CO^{2+} dication. The total KER spectrum in Fig. 1(d) shows that the sequential fragmentation leads to lower KER than the concerted fragmentation. This can be qualitatively interpreted as resulting from the population of higher excited states of the CO^{2+} dication for the concerted fragmentation events than for the sequential ones.

Three processes have thus been identified: a concerted fragmentation process corresponding to the population of dissociative or very-short-lifetime states of the CO^{2+} dication, a sequential fragmentation process corresponding to the population of metastable states with lifetimes significantly shorter than 2.7 μs , and the population of metastable states with lifetimes longer than 2.7 μs whose dissociation could not be directly observed experimentally.

B. Simulations

In order to quantitatively determine the range of lifetimes associated with the sequential process, numerical simulations based on a simple classical model have been performed. This model was used beforehand to determine the geometry of $(\text{CO})_2$ dimers using the concerted fragmentation events and is described in detail in [10]. Briefly, the triply ionized dimer is initially represented as three fixed in space and pointlike particles with the respective charges and masses of CO^+ , C^+ , and O^+ , where the C^+ and O^+ ions compose the dissociating CO^{2+} dication with a bond length of 1.13 Å. Following the conclusions obtained in [10], the mean intermolecular

distance between the two covalent molecules is set to $R = 4.2$ Å. The mean angle between the dimer axis and the CO^{2+} molecular axis is set to $\theta_i = 90^\circ$, where θ_i gives the direction of the carbon atom and $\theta_i + 180^\circ$ the direction of the oxygen atom. Although the initial orientation of the CO^{2+} with respect to the dimer axis is expected to be isotropic [10], the angle θ_i is here fixed at 90° to ease the interpretation of the simulation. We will show later that this simplification does not change the overall conclusions. As in [10], the simulation also accounts for jitters on the mean value of R .

For the first step of the fragmentation, we only consider a pure Coulombic two-body fragmentation of the dimer and compute the trajectories of two pointlike molecular ions CO^{2+} and CO^+ , up to a time t . The duration t of the first step depends on the chosen decay constant τ of the CO^{2+} dication and follows a probability distribution $P(t) = \alpha e^{-t/\tau}$. The equations of motion are integrated using a standard Runge-Kutta method and assuming a pure Coulomb repulsion between the two molecular ions.

The subsequent dissociation of the CO^{2+} dication is then simulated in a similar way but with a three-body interaction between the C^+ , O^+ , and CO^+ ions. In this second step, the CO^{2+} dication dissociates at a distance d from the CO^+ molecular ion which depends on the decay time t and with a new orientation angle θ_f to account for the free rotation of the CO^{2+} molecular ion's prior dissociation. The angle θ_f between the initial dimer axis and the CO^{2+} molecular ion is simply given by $\theta_f = \theta_i + 2\pi t/T_{\text{rot}}$, where T_{rot} is the rotation period of the CO^{2+} molecule. The value of T_{rot} is set to 0.98 ps, which corresponds to the rotation period obtained within a classical calculation by solving the equation of motion of the first step, approximating the CO^{2+} molecular ion by a C^+ ion and a O^+ ion linked by a 1.13-Å-long rigid bound. Within this approximation, the CO^{2+} rotation takes place in the initial plane containing both the center of mass of the CO^+ ion and the axis of the $(\text{CO})^{2+}$ dication and is due to the lower mass of the carbon compared to oxygen, leading to a stronger acceleration of the carbon site.

As shown in Fig. 1(d), the concerted fragmentation and the sequential fragmentation differ by the final KER distributions associated with each process. To reproduce in the simulation the KER distribution expected for sequential fragmentation events, a non-purely-Coulombic repulsion between the C^+ and O^+ ions from the dissociating CO^{2+} dication is accounted for by a scaling of the repulsive force [10]. This non-Coulombic repulsion is directly inferred from the experimental KER spectrum for sequential events.

The evolution of the mean kinetic energy of the CO^+ molecular ion as a function of the time t during the first step is plotted in Fig. 2 for the sequential fragmentation. The asymptotic energy of 3.2 eV corresponding to the peak observed in Fig. 1(c) is reached for t values ranging from approximately 1 ps to 10 ps, which indicates that sequential fragmentation events correspond to a fragmentation time t larger than 1 ps. A clearer picture can be obtained by looking at the simulations' Dalitz plots shown in Fig. 3. For $\tau < 2$ ps, one can clearly see the Dalitz distribution moving first towards higher values of y_D , which corresponds to higher transfer momentum to the CO^+ ion. Then it expands to the right (higher momentum transfer to the O^+ ion) due to the

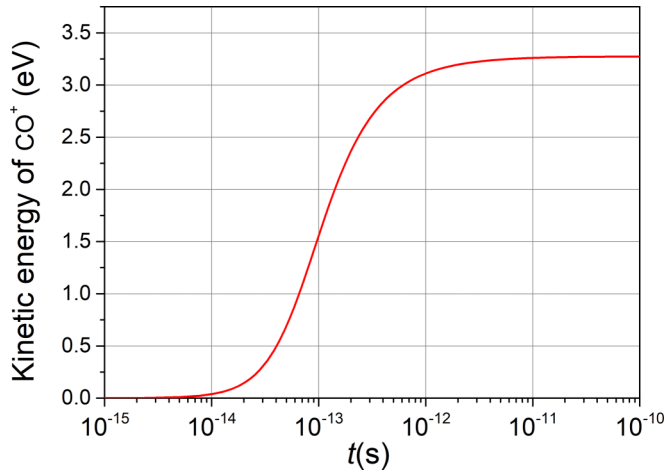


FIG. 2. Evolution of the mean kinetic energy of the CO^+ molecular ion as a function of time t in the first step of the sequential fragmentation: two-body dissociation $(\text{CO})_2^{3+} \rightarrow \text{CO}^{2+} + \text{CO}^+$.

rotation of the CO^{2+} molecular ion. For lifetimes larger than 500 fs, the angle θ_f reaches 270° and the left part of the Dalitz distribution (higher momentum transfer to the C^+ ion) is also filled, forming the quasihorizontal band observed in

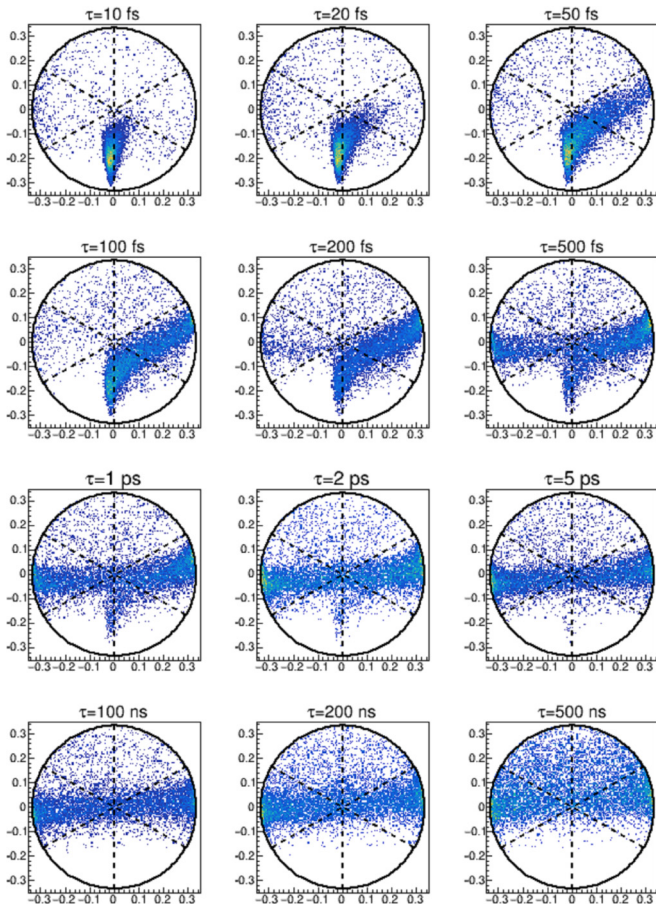


FIG. 3. Dalitz plots obtained with the Monte Carlo simulations of the sequential fragmentation process for different lifetimes τ of the CO^{2+} dication.

the experimental data. Within this time sequence between 50 fs and 1 ps, the fact that the right side of the horizontal band is filled before the left side arises from our choice to fix θ_i at 90° . Starting with an isotropic orientation of the CO^{2+} molecular ion within the dimer would simply result in the simultaneous filling of both sides of the band. The quasihorizontal band is finally clearly obtained without deformation (no remaining events for $y_D < 0$) for dissociation lifetimes larger than ~ 2 ps and remains unchanged up to ~ 200 ns. For large dissociation times t , the reconstruction of the fragments' momenta should start to fail, the duration of the first step being neglected in the data analysis procedure. The present simulations show that for times up to 200 ns, the reconstruction of the momentum vectors of the C^+ and O^+ ions remains accurate enough to provide the same pattern on the Dalitz plot as for a 2-fs dissociation time. For dissociation times larger than 200 ns, the quasihorizontal band becomes thicker and the upper part of the Dalitz plot, above the band, start to be filled with events. This last change in the Dalitz figure arises when the CO^{2+} fragmentation occurs at a distance d that is sufficiently far away from the collision region to prevent a proper reconstruction of the fragment momenta. The sequential process observed experimentally in Fig. 1(a) can thus be attributed to the population of metastable states of the CO^{2+} molecular ion with lifetimes comprised between about 2 ps and 200 ns. The same simulations have been performed using the concerted fragmentation KER distribution. They have shown that for events identified with the concerted fragmentation selection window of Fig. 1(a), the van der Waals and covalent bonds break apart within less than 10 fs. As can be seen in Fig. 2, this also corresponds to times that are too short to allow a significant acceleration of the CO^+ molecular ion.

We did not observe here metastable states with lifetimes of the order 100 fs, but the technique could be particularly suitable to investigate such states. If the CO^{2+} fragmentation takes place for $t \sim 100$ fs, the two molecular ions are not sufficiently far away to reach the asymptotic part of Fig. 2 and the resulting Dalitz plots would show specific patterns as in Fig. 3 for t ranging from 50 to 500 fs. The detailed study of such Dalitz plots could then give access to a more precise estimate of the lifetime. Note that the present range of 50–500 fs is specific to the present fragmentation system. For molecular dimers of different internuclear or intermolecular distances and fragment ions of different masses, this range would be shifted. Another specificity of the molecular system investigated here is the initial quasi-isotropic angular distribution of the CO molecules within the dimer, which prevents the use of information carried through fragment angular correlations. With a well-defined initial orientation of the molecules, subrotational lifetimes of the molecular ions could also be accessed more directly using the so-called native frame approach, as recently demonstrated for SO^{2+} ions resulting from SO_2^{3+} ions fragmentation [14].

C. Identification of the metastable states

As already described in a previous study on nitrogen dimers $(\text{N}_2)_2$ [13], the total KER of the three-body channels (sum of the kinetic energy of the three emitted fragments) can be compared to the KER spectrum of the dication dissociation

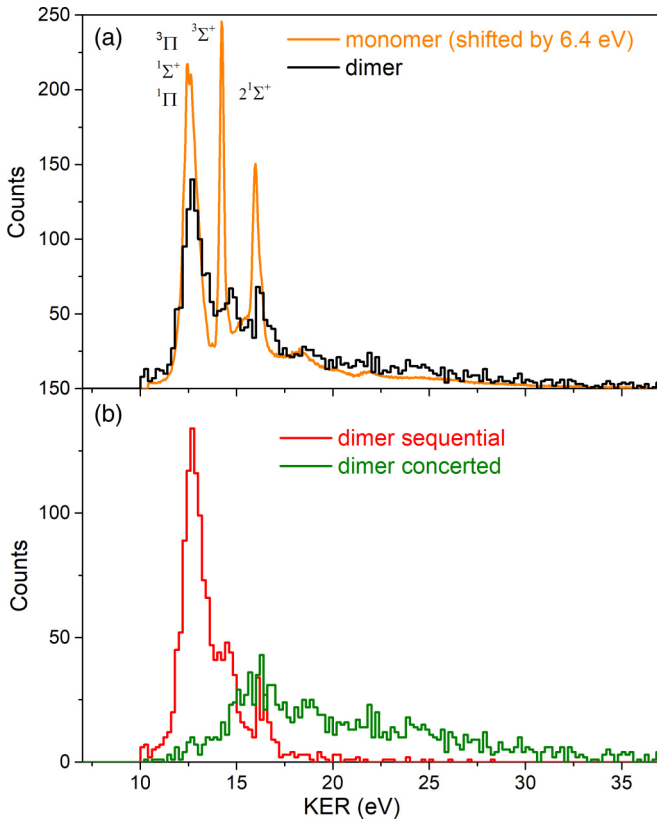


FIG. 4. (a) Total KER spectrum for the $(\text{CO})_2^{3+} \rightarrow \text{CO}^+ + \text{C}^+ + \text{O}^+$ fragmentation channel (black line) and KER spectrum of the $\text{CO}^{2+} \rightarrow \text{C}^+ + \text{O}^+$ fragmentation of monomer targets shifted by 6.4 eV [orange (light gray) line]. The KER spectrum obtained for dimers is normalized to the one obtained with dimers. (b) Contributions of the sequential fragmentation [red (gray) line] and concerted fragmentation events [green (light gray) line] after a data selection performed using the selection windows of Fig. 1(a).

from monomer targets by simply accounting for the extra kinetic energy resulting from the pure Coulomb repulsion with the neighbor molecular ion. Such a comparison is provided in Fig. 4(a) for $(\text{CO})_2$ dimers. For the three-body dissociation channel, assuming $R_e = 4.2 \text{ \AA}$ and a pure Coulomb model, the expected energy shift is $\Delta\text{KER} = 6.4 \text{ eV}$ and agrees perfectly with our measurement.

The global shape of the total KER spectrum (black line) is quite similar to the KER distribution obtained with the monomer CO target (orange line). Three peaks at low energy are clearly visible for the dimer, although they are not as well resolved as for the monomer. This larger width of the peaks can be explained by the additional jitter in total KER due to the vibrational motion of the dimer bond. Following the identification from [15], the first peak at 6.2 eV corresponds to the population of the ${}^3\Pi$, ${}^1\Sigma^+$, and ${}^1\Pi$ states, the second one at 7.8 eV to the ${}^3\Sigma^+$ state, and the third one at 9.6 eV to the $2^1\Sigma^+$ state. Other high-lying states leading to a wide KER distribution between 17 and 35 eV are also populated for both the dimer and the monomer targets. Small differences can nevertheless be observed between dimer and monomer targets when looking closely at the relative population of the different molecular states. With dimer targets, values of KER higher

than 17 eV are favored while lower KER values (corresponding in particular to the ${}^3\Sigma^+$ and $2^1\Sigma^+$ states) are disfavored. As both collision systems are investigated simultaneously with the same setup and thus with the same acceptance, this is a signature of a difference mainly resulting from the primary collision process. The removal of three electrons from the dimer target (two from one of the CO molecules and one from its neighbor) requires smaller impact parameters than the removal of two electrons from a single CO molecule. In the case of dimer targets, this leads to a larger population of high excitation states (from 17 to 35 eV) and to a smaller population of the ground and low-lying states corresponding to the three peaks in KER lying between 10 and 17 eV. It also clearly appears [Fig. 4(b)] that the sequential fragmentation is only associated with the lower-energy part of the KER spectrum whereas concerted fragmentation occurs mainly for higher KER values.

For the events corresponding to a sequential fragmentation, the dissociation of CO^{2+} occurs far enough from the CO^+ partner to be directly compared with the dissociation of a CO^{2+} dication originating from a monomer. For this purpose, the sum of the kinetic energy of the C^+ and O^+ ions can be calculated in the frame of the center of mass of the transient recoiling CO^{2+} molecular ion. As the momenta of the CO^{2+} and CO^+ are equal but have opposite directions, the corresponding momentum vectors in the recoiling center-of-mass frame are

$$\vec{p}_{\text{C}^+}^* = \vec{p}_{\text{C}^+} + \frac{m_{\text{C}}}{m_{\text{CO}}} \vec{p}_{\text{CO}^+},$$

$$\vec{p}_{\text{O}^+}^* = \vec{p}_{\text{O}^+} + \frac{m_{\text{O}}}{m_{\text{CO}}} \vec{p}_{\text{CO}^+}.$$

The total kinetic energy of the two atomic ions in this frame is given by

$$\text{KE}^* = \frac{\|\vec{p}_{\text{C}^+}^*\|^2}{2m_{\text{C}}} + \frac{\|\vec{p}_{\text{O}^+}^*\|^2}{2m_{\text{O}}}.$$

The KE^* spectrum for the sequential fragmentation events is shown in Fig. 5 along with the KER spectrum obtained with CO monomers. The use of the KE^* observable allows a clearer comparison with the monomer as it directly provides the kinetic energy released in the dissociation of the CO^{2+} transient dication. Note that this observable is only meaningful for sequential fragmentation events: If the CO^{2+} dissociation occurs too close to the neighbor CO^+ ion, the dissociation must be treated as a real three-body process. The peaks in KE^* displayed in Fig. 5 are now well resolved because the KE^* spectrum does not depend on the initial dimer bond length (asymptotic energy of the CO^+ ion). Figure 5 allows us to confirm the previous identification of the populated states. The peaks respective mean positions are very close to the ones obtained with the monomer target, but for the ${}^3\Sigma^+$ and $2^1\Sigma^+$ states, they are clearly shifted by $\sim 0.1\text{--}0.2 \text{ eV}$. Again, as both collision systems with dimer and monomer targets are investigated simultaneously in a single experiment and as we use the same analysis procedure (with identical calibration), this shift cannot be imputed to an experimental bias. Such a shift was observed in a previous work [9] and was attributed to the fact that within the first step of the fragmentation, when the van der Waals bond is broken, a small part of the energy is transferred

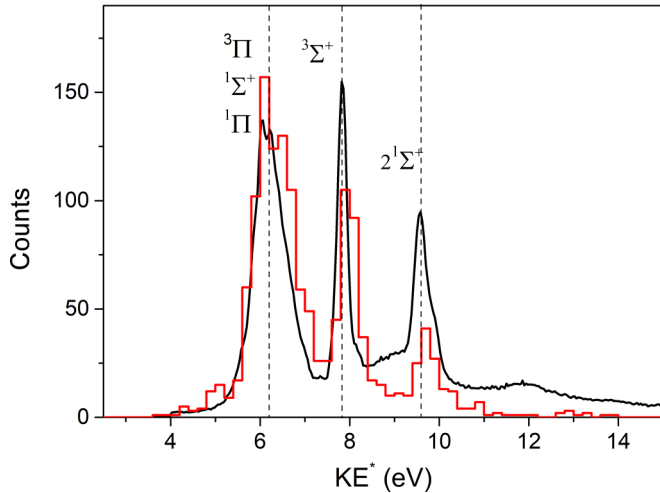


FIG. 5. Sum of the kinetic energy of the C^+ and O^+ ions calculated in the center of mass of the CO^{2+} transient ion for the sequential fragmentation event selection [red (gray) line]. The KER spectrum results from collisions with monomer targets (black line). The KER spectrum obtained for monomers is normalized to the one obtained with dimers in the range between 4 and 11 eV. One bin corresponds to 0.2 eV on the spectrum obtained with dimers.

to the CO^{2+} dication to populate higher vibrational states. The KER obtained for the monomer indicates that for the $^3\Sigma^+$ and $2^1\Sigma^+$ states, the lowest vibrational level $\nu = 0$ is dominantly populated. The shift of ~ 0.2 eV observed for these states when using dimer targets can thereby be explained by a population transfer due to the van der Waals bond breakup from the $\nu = 0$ levels towards the $\nu = 1$ levels lying at respectively 0.26 and 0.29 eV higher energies.

In the present experiment, we identified the population of molecular states of the CO^{2+} dication associated with a sequential fragmentation of the dimer target: the manifolds of the $^3\Pi$, $^1\Sigma^+$, and $^1\Pi$ states and the $\nu = 0$ and $\nu = 1$ vibrational levels of the $^3\Sigma^+$ and $2^1\Sigma^+$ states. The analysis of the Dalitz plots of Fig. 3 for this sequential process have shown that all these molecular states have lifetimes in the 2 ps to 200 ns range, which is in agreement with the previous measurements and calculations provided in Table I.

D. Fast dissociation channels

Concerted fragmentation occurs only for KER values higher than 12 eV and spreading up to 35 eV [Fig. 4(b)]. These KER values can be attributed to the population of excited states of the CO^{2+} dication with dissociative potential energy curves or with lifetimes shorter than 10 fs, leading to a quasisimultaneous breakup of the van der Waals and covalent bonds. The lower-energy part of the KER spectrum for concerted fragmentation events overlaps with the $2^1\Sigma^+$ state manifold identified in the sequential selection. However, the very fast dissociation time observed for this concerted process implies that this part of the KER distribution arises from different initial molecular electronic (or vibrational) states.

It is important to note that the large tail in KER between 17 and 35 eV is also observed in the KER spectrum obtained with monomer targets when accounting for the 6.4-eV shift in KER

TABLE I. KER and lifetimes of the ground state and low-lying states of the CO^{2+} monomer dication. Theoretical lifetimes are extracted from Fig. 1 of [6].

State	Vibrational		Lifetimes	
	level	KER (eV) ^a	Expt.	Calc. ^b
$^3\Pi$	0, 1		$> 10 \mu s^c$	> 1 s
$^3\Pi$	2	5.6	200 ns ^c	800 ns
$^3\Pi$	3	5.8	< 100 ns ^c	1 ns
$^3\Pi$	4–11	6.0–6.8	10 fs–50 ns ^a	10 ps–1 ns
$^3\Pi$	≥ 12			< 1 ps
$^1\Sigma^+$	0		$> 10 \mu s^c$	20 s
$^1\Sigma^+$	1	5.7	700 ns ^c	100 μs
$^1\Sigma^+$	2	6.0		500 ns
$^1\Sigma^+$	3			80 ns
$^1\Sigma^+$	4–23			10 ps–1 ns
$^1\Sigma^+$	≥ 24			< 1 ps
$^1\Pi$	0	5.8	200 ns ^c	7 μs
$^1\Pi$	1	6.0	< 100 ns ^c	10 ns
$^1\Pi$	2–10	6.2–7.5	10 fs–50 ns ^a	10 ps–1 ns
$^1\Pi$	≥ 23			< 1 ps
$^3\Sigma^+$	0	7.8	10 fs–50 ns ^a	10 ns
$^3\Sigma^+$	1	8.1	10 fs–50 ns ^a	1 ns
$^3\Sigma^+$	2–6	> 8.3		10 ps–1 ns
$2^1\Sigma^+$	0	9.5	10 fs–50 ns ^a	
$2^1\Sigma^+$	1	9.8	10 fs–50 ns ^a	

^aReference [15].

^bReference [6].

^cReference [3].

[Fig. 4(a)]. This indicates that such excited states leading to fast molecular dissociation are also populated in the collisions with monomer targets. It is thus found in contradiction with the conclusions of the former work of Ding *et al.* using short laser pulse ionization [9]. In this previous study, the low-lying states $^3\Pi$, $^1\Sigma^+$, and $^1\Pi$ of CO^{2+} were dominantly populated for both the dimer and monomer targets. When compared to the KER obtained with monomer targets, the KE^* distribution of the sequential fragmentation process was found almost identical. However, the KER distribution obtained with dimers for the fast dissociation process was found to be ~ 1 eV higher than for the sequential fragmentation. This fast process was then interpreted as resulting from the presence of a neighbor CO^+ ion in the dimer inducing a symmetry breaking of the $^3\Pi$ state. Indeed, their calculations of potential energy curves accounting for the presence of the neighbor CO^+ ion revealed a fragmentation pathway involving both an avoided crossing with the dissociative $^3\Sigma^-$ state and the appearance of a new electronic state, leading to a final KER higher by 1.2 eV. They concluded that the fast dissociation process was only enabled by the presence of the neighbor ion and that this fast process should not be expected with CO^{2+} dications from a monomer target.

The results obtained in our experiment are similar in two aspects: We only observe sequential fragmentation for KER values below 17 eV ($^3\Pi$, $^1\Sigma^+$, and $^1\Pi$ states of CO^{2+}) and a higher KER distribution for concerted dissociation than for sequential dissociation. However, the KER spectrum of

the present work for concerted fragmentation is much wider (extending up to 35 eV) with a maximum of the distribution peaking at 16.5 eV. This KER distribution cannot be explained by the relaxation process invoked previously in [9]. First, the shift in KER between the maxima of the distributions obtained for concerted and sequential processes is close to 4 eV, which is much higher than the value of 1.2 eV predicted in [9]. Moreover, the tail between 17 and 35 eV obtained for the concerted fragmentation is also observed with monomer targets [Fig. 4(a)], which demonstrates that the process leading to such KER values is not due to the presence of a neighbor ion. The higher KER values obtained here must thus arise from the direct population of high-lying excited states leading to fast dissociation.

Several conclusions can be drawn from these observations. Collisions with highly charged ions lead to the population of higher excited states of the CO^{2+} dication than with short laser pulses, for both dimer and monomer CO targets. The population of highly excited states could even be enhanced at higher collision energy, as previously observed in [16]. While the $^3\Pi$, $^1\Sigma^+$, and $^1\Pi$ states of CO^{2+} show lifetimes systematically larger than 2 ps, higher excited states all lead to fast dissociation. As such excited states were observed both with dimer and monomer targets, this fast dissociation process is not dependent on the presence of a neighbor ion and fast dissociation must also occur with monomer CO targets. Finally, the present observations confirm the conclusions obtained in [13] for the study of the fragmentation of $(\text{N}_2)_2$ dimers, showing no evidence for a significant effect of the neighbor molecular ion besides the shift in KER due to the Coulomb repulsion.

IV. CONCLUSION

Beyond providing information on the geometry of van der Waals molecular clusters, COLTRIMS and CEI turn out to be smart tools to probe the lifetimes of the molecular states populated in collisions with highly charged ions. For the three-

body fragmentation channel $(\text{CO})_2^{3+} \rightarrow \text{CO}^+ + \text{C}^+ + \text{O}^+$, about half of the events have been assigned to a sequential dissociation resulting from the population of metastable states of the CO^{2+} dication with lifetimes between 2 ps and 200 ns. These states result in low KER values and are associated with low excited states of the dication, namely, the $^3\Pi$, $^1\Sigma^+$, and $^1\Pi$ states, and the $\nu = 0$ and $\nu = 1$ vibrational levels of the $^3\Sigma^+$ and $2^1\Sigma^+$ states. In a more general way, this experimental approach provides opportunities to get insight into dication molecular states and their associated lifetimes. The present technique would indeed be particularly well suited for the study of metastable states with lifetimes of the order of 100 fs, where a more precise lifetime estimate could be obtained. With dimer targets produced with low rotational energy and with a well-known initial molecular orientation, this technique would also provide access to the measurement of any subrotational lifetime of molecular dications using the native frame representation, as recently performed in [14].

In the present work, the population of higher excited states leading to a prompt dissociation and to a concerted fragmentation of the dimer was also clearly evidenced. The analysis of the KER distribution for this process has shown that the fast dissociation cannot be explained by the effect of the neighbor molecular ion. Contrarily, the similarity between the KER spectra obtained for dimer and monomer targets indicates the population of fast dissociating states in collisions with monomer targets. Altogether, this analysis shows a negligible effect of the neighbor molecular ion in the relaxation process of the $(\text{CO})_2^{3+}$ system.

ACKNOWLEDGMENTS

The experiment was performed at the Grand Accélérateur National d'Ions Lourds (GANIL) by means of the CIRIL Interdisciplinary Platform, part of CIMAP Laboratory, Caen, France. The authors want to thank the CIMAP and GANIL staff for their technical support.

-
- [1] E. Friedländer, H. Kallmann, W. Lasareff, and B. Rosen, *Z. Phys.* **76**, 60 (1932).
 - [2] L. H. Andersen, J. H. Posthumus, O. Vahtras, H. Ågren, N. Elander, A. Nunez, A. Scrinzi, M. Natiello, and M. Larsson, *Phys. Rev. Lett.* **71**, 1812 (1993).
 - [3] F. Penent, R. I. Hall, R. Panajotović, J. H. D. Eland, G. Chaplier, and P. Lablanquie, *Phys. Rev. Lett.* **81**, 3619 (1998).
 - [4] J. P. Bouhnik, I. Gertner, B. Rosner, Z. Amitay, O. Heber, D. Zajfman, E. Y. Sidky, and I. Ben-Itzhak, *Phys. Rev. A* **63**, 032509 (2001).
 - [5] R. W. Wetmore, R. J. Le Roy, and R. K. Boyd, *J. Chem. Phys.* **88**, 6318 (1984).
 - [6] F. Mrugała, *J. Chem. Phys.* **129**, 064314 (2008).
 - [7] T. Šedivcová, P. R. Žďánská, and V. Špirko, *J. Chem. Phys.* **124**, 214303 (2006).
 - [8] A. Pandey, B. Bapat, and K. R. Shamasundar, *J. Chem. Phys.* **140**, 034319 (2014).
 - [9] X. Ding, M. Haertel, S. Schlauderer, M. S. Schuurman, A. Y. Naumov, D. M. Villeneuve, A. R. W. McKellar, P. B. Corkum, and A. Staudte, *Phys. Rev. Lett.* **118**, 153001 (2017).
 - [10] A. Méry, V. Kumar, X. Fléchar, B. Gervais, S. Guillous, M. Lalande, J. Rangama, W. Wolff, and A. Cassimi, *Phys. Rev. A* **103**, 042813 (2021).
 - [11] P. Song, X. Wang, C. Meng, W. Dong, Y. Li, Z. Lv, D. Zhang, Z. Zhao, and J. Yuan, *Phys. Rev. A* **99**, 053427 (2019).
 - [12] J. Rajput, T. Severt, B. Berry, B. Jochim, P. Feizollah, B. Kaderiya, M. Zohrabi, U. Ablikim, F. Ziaee, Kanaka Raju P., D. Rolles, A. Rudenko, K. D. Carnes, B. D. Esry, and I. Ben-Itzhak, *Phys. Rev. Lett.* **120**, 103001 (2018).
 - [13] A. Méry, A. N. Agnihotri, J. Douady, X. Fléchar, B. Gervais, S. Guillous, W. Iskandar, E. Jacquet, J. Matsumoto, J. Rangama, F. Ropars, C. P. Safvan, H. Shiromaru, D. Zanuttini, and A. Cassimi, *Phys. Rev. Lett.* **118**, 233402 (2017).
 - [14] J. Rajput, H. Kumar, P. Bhatt, and C. P. Safvan, *Nat. Sci. Rep.* **10**, 20301 (2020).
 - [15] M. Lundqvist, P. Baltzer, D. Edvardsson, L. Karlsson, and B. Wannberg, *Phys. Rev. Lett.* **75**, 1058 (1995).
 - [16] M. Tarisien, L. Adoui, F. Frémont, D. Lelièvre, L. Guillaume, J.-Y. Chesnel, H. Zhang, A. Dubois, D. Mathur, S. Kumar, M. Krishnamurthy, and A. Cassimi, *J. Phys. B* **33**, L11 (2000).